

# Mitigation of Cross-Saturation Effects in Resonance-Based Sensorless Switched Reluctance Drives

K.R. Geldhof, A. Van den Bossche and J.A.A. Melkebeek

Department of Electrical Energy, Systems and Automation (EESA)

Ghent University (UGent), Sint-Pietersnieuwstraat 41, B-9000 Gent, Belgium

phone: +32 (0)9 264 3442, fax: +32 (0)9 264 3582

e-mail: Kristof.Geldhof@UGent.be

**Index Terms**—Switched Reluctance Machines, Cross-Saturation, Position Estimation, Resonance, Test Pulse

**Abstract**—The stator and rotor yoke in a switched reluctance motor form magnetic circuit parts that are typically shared by different phases. If these parts saturate due to the excitation of one phase, this will lead to a change of the magnetic characteristics of all other phases sharing these parts. In several position-sensorless methods, cross-saturation leads to a load-dependent position estimation error. In this paper, the influence of cross-saturation on a resonance-based position estimation method is studied. The method extracts position information from electrical resonances triggered in an idle motor phase. A cross-saturation mitigation scheme is presented in order to reduce the commutation position error. The scheme uses only one additional parameter per phase which can be measured automatically during commissioning of the drive. Experimental results at low and medium speed show that the position estimation error remains smaller than 2 mechanical degrees over the rated load range.

## I. INTRODUCTION

In several position-sensorless methods for switched reluctance motors (SRMs), it is recognized that mutual coupling between motor phases has to be taken into account in order to achieve good position estimation.

A sensorless method that is inherently based on mutual coupling is presented in [1]. The position estimation is based on the measurement of mutually induced voltages in an idle phase of the machine.

In [2] an estimator probes idle phases with short voltage pulses from the inverter. From the resulting current response the incremental phase inductance can be estimated. The mutually induced voltage changes the slope of the current response and leads to a position estimation error. A compensation can be provided on the basis of a look-up table.

The flux/current method originally proposed in [3] calculates the flux linkage of the active phase by time integration of the induced voltage. The rotor position is retrieved from a single-phase magnetization characteristic, stored in a look-up table. In case of multi-phase excitation, mutual coupling can be taken into account if the look-up table incorporates the current of all excited phases. Alternatively, a weighted sum of self flux linkage and mutual flux linkage data can be used to

enhance position estimation; the weight factor depends on the currents in the excited phases [4].

All of these methods take into account the stator pole-to-pole leakage, which is the principle source of mutual coupling between switched reluctance motor phases. A secondary source of mutual coupling is cross-saturation, i.e. the saturation of magnetic circuit parts which are shared by different phases. It has been identified that in the case of multi-phase excitation, cross-saturation can be a means to increase the average torque [5]. However, cross-saturation has not often been identified as a possible problem in sensorless switched reluctance drives. In one occasion cross-saturation is taken into account by means of a complex lumped-parameter model of the machine [3].

This paper discusses the influence of cross-saturation on a resonance-based sensorless method for SRMs [6]. If the trailing phase with respect to the torque-producing phase is used to extract position information, the position error leads to an advanced phase commutation. A mitigation scheme is presented that uses only one additional parameter per phase which can be easily measured during commissioning of the drive. Application of the scheme leads to a significantly reduced error in the estimated commutation position. Experimental results are given for low and medium speed, for the rated load range of a 6x4 switched reluctance motor.

## II. RESONANCE-BASED POSITION ESTIMATION

In switched reluctance drives, the rotor position can be obtained by observation of the oscillation of a resonant circuit comprising the inductance and parasitic capacitance associated with an idle motor phase [6]. Fig. 1(a) shows a schematic of a motor phase winding connected to an asymmetric bridge, with IGBTs as active switching devices. If the IGBTs and freewheeling diodes are blocked, these devices behave as a parasitic capacitance. The model of Fig. 1(b) shows these parasitic capacitances, indicated by  $C_i$  and  $C_d$  respectively, and the parasitic capacitance  $C_w$  of the motor phase winding and the capacitance  $C_c$  associated with the power cable between converter and motor phase. The impedance  $Z_w$  represents the phase winding impedance without the contribution of the parasitic capacitance  $C_w$ .

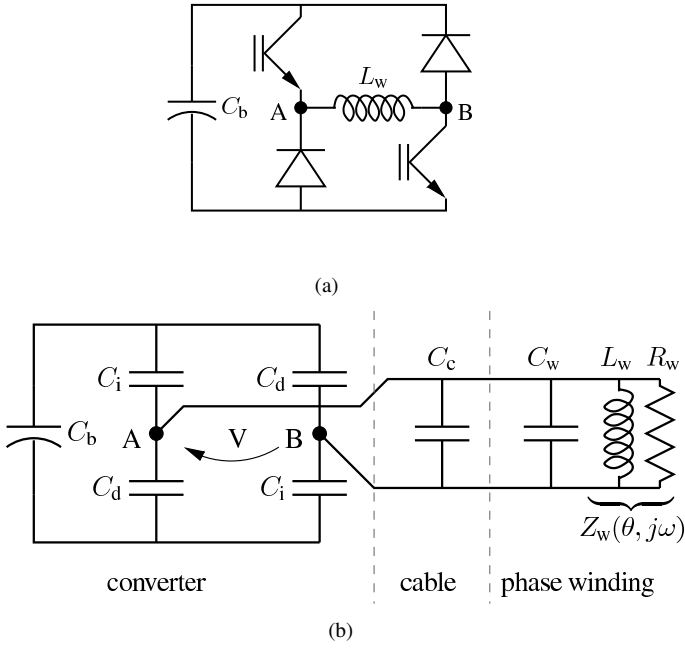


Figure 1. Converter H-bridge with phase winding (a) and parasitic model of motor-converter combination (b).

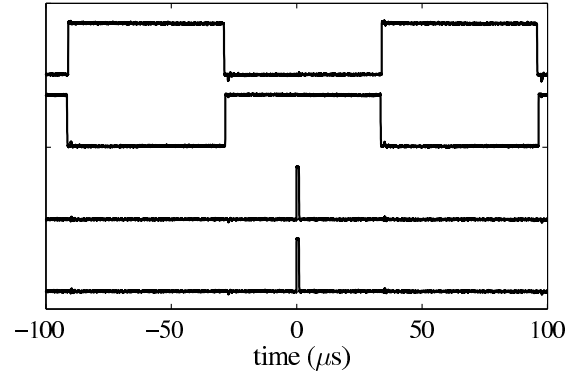
The circuit of Fig. 1(b) can be excited by application of a short voltage pulse, see Fig. 2(a). During the short switch-on of the IGBTs, the parasitic capacitances  $C_d$ ,  $C_c$  and  $C_w$  are charged up to the bus bar voltage  $V_{dc}$ . At the end of the voltage pulse, a resonance is initiated due to an exchange of energy between the parasitic capacitances and the phase inductance  $L_w$ . The resonance can be observed in the phase voltage and is shown in Fig. 2(b) for two positions of the 6x4 SRM used in the experimental set-up. The resonances are damped, mainly due to eddy currents in the magnetic material. Most importantly, the resonances shows a strong position-dependence. If the rotor is in the aligned position with respect to the test phase, the phase inductance has a maximum value and the corresponding (undamped) resonance frequency will reach a minimum value, given by

$$\omega_{\text{res}} = \frac{1}{\sqrt{L_w(\theta, \omega_{\text{res}})C_{\text{eq}}}}, \quad (1)$$

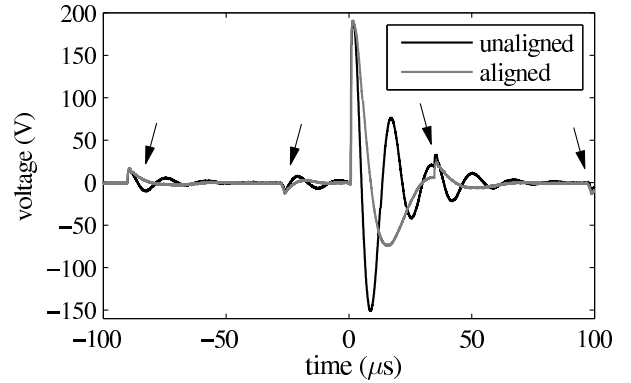
where  $C_{\text{eq}}$  represents the total equivalent parasitic capacitance:

$$C_{\text{eq}} = \frac{C_i + C_d}{2} + C_c + C_w. \quad (2)$$

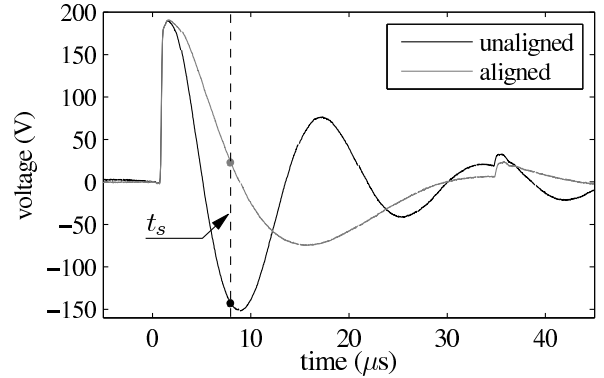
It can be seen from Fig. 2 that the timing of the test pulse is chosen in such a way that the first two oscillation periods of the resonance waveform are not disturbed by the switching actions in the active (torque-producing) phase. Moreover, the mutually induced voltage in the test phase is negligible due to the fact that the test pulse is generated during a freewheeling period in the active phase: only one of the IGBTs of the active phase is switched on when the test pulse is applied in the idle phase, see Fig. 2(a). Therefore the principal source of mutual coupling, i.e. the pole-to-pole leakage flux, has no effect on the



(a) Control signals for IGBTs of phase B (top) and IGBTs of phase C (bottom).



(b) Voltage resonance in phase C. The arrows indicate distortions due to switching actions in phase B.



(c) Detail of (b). The resonance is sampled at time  $t_s$ .

Figure 2. Application of a  $1 \mu\text{s}$  voltage pulse in phase C, for the unaligned and aligned position of the rotor with respect to phase C. Phase B is PWM current-controlled, with  $i_b = 1 \text{ A}$ . The bus bar voltage  $V_{dc}$  equals 200 V.

position estimation, at least at relatively low speeds. At high speeds the speed-induced emf becomes large and consequently a large duty ratio has to be applied to the active phase. For high duty ratios the freewheeling interval within a PWM period is strongly reduced, eliminating the possibility to impose test pulses in this interval. The solution for high-speed operation falls out of the scope of this paper. In the following, only low-speed and medium-speed operation will be discussed.

If the phase voltage resonances are measured at a fixed time  $t_s$  relative to the start of each pulse, each voltage sample can be mapped to the rotor position at which the sample was measured. As a consequence, the measured voltage samples form a position signature of the combination of motor phase and converter. Fig. 3 shows the measured signatures  $v_{sA}$ ,  $v_{sB}$  and  $v_{sC}$  of the three motor phases, for the chosen sample time  $t_s$  as indicated in Fig. 2(c). The maxima of each position signature in Fig. 3 correspond to aligned positions with respect to the phase, while the minima correspond to unaligned positions.

For low speed, the grey area in Fig. 3 indicates the position interval  $[26^\circ-56^\circ]$  in which phase  $B$  is excited in order to generate motoring torque. With the help of Fig. 2(c), it can be deduced that the regions of rising inductance (decreasing resonance frequency) correspond with regions of rising voltage samples<sup>1</sup>.

In the SRM under test, the rotation direction which leads to an increase in the rotor angle corresponds to the phase excitation sequence  $C \rightarrow B \rightarrow A \rightarrow C \rightarrow \dots$ . During excitation of phase  $B$ , test pulses can be applied to phase  $A$  or phase  $C$ , which are the leading and trailing phase respectively for this rotation direction. The end of the excitation, i.e. the commutation instant, is determined on the basis of the measured voltage sample in the test phase. If phase  $A$  is used, commutation is performed when  $v_{sA}$  crosses the threshold  $v_{tA}$ . If phase  $C$  is used, commutation is performed when  $v_{sC}$  crosses the threshold  $v_{tC}$ . Both cases are shown in Fig. 3.

In the vicinity of the commutation angle  $56^\circ$ , the position signatures of  $A$  and  $C$  show more or less the same sensitivity with respect to a rotor position variation. From this point of view, there is no preference whether to use the leading or trailing phase as a test phase. For increasing speed however, it is usual to perform phase advance in order to compensate for the finite rise time of the current when a phase is excited. In Fig. 3, a phase advance corresponds to a shift of the indicated position interval (the grey rectangle) to the left. Correspondingly, the commutation angle decreases. For a phase advance of  $8^\circ$  or more, it can be seen that  $v_{sA}$  shows a very small angle sensitivity, as the commutation instant is situated near the unaligned position with respect to phase  $A$ . Therefore, the trailing phase  $C$  is the better choice to use as test phase. Only if the phase advance would exceed  $14^\circ$ , a switch-over should be made from the trailing phase to the leading phase in order to maintain sufficient position sensitivity.

<sup>1</sup>This is a valid conclusion as long as  $t_s$  is smaller than the time instant at which the unaligned voltage resonance reaches its minimum.

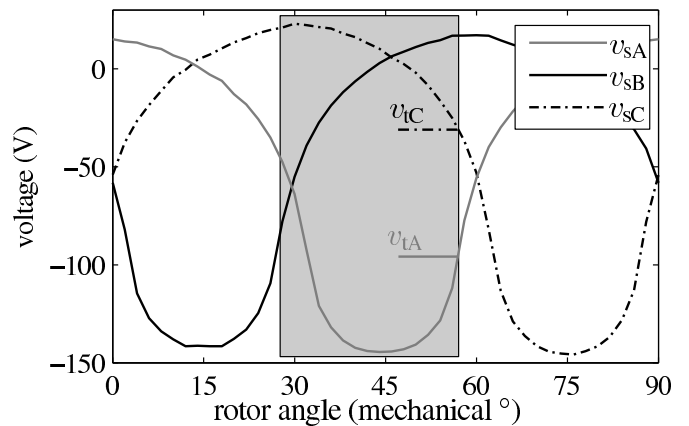


Figure 3. Measured position signatures  $v_{sA}$ ,  $v_{sB}$ ,  $v_{sC}$  of motor phases  $A$ ,  $B$ ,  $C$ . The grey area indicates the excitation region for phase  $B$  in the case of low-speed motoring operation. The voltage level  $v_{tA}$  or  $v_{tC}$  is used as commutation threshold if phases  $A$  or  $C$  are used as respective test phases.

In the following, the trailing phase with respect to the active phase is chosen as the test phase.

### III. INFLUENCE OF CROSS-SATURATION

In a conventional switched reluctance machine, phases share a common magnetic path in the stator and rotor yoke. If these paths saturate partly or completely due to the excitation of an active phase, this results in an increased magnetic reluctance for the other phase as well. The influence of cross-saturation is investigated on the experimental set-up by applying at fixed rotor positions different levels of current in phase  $B$ , while triggering voltage resonance in phase  $C$ . If the voltage waveforms are measured at time  $t_s$  as indicated in Fig. 2(c), the resulting position signatures of Fig. 4 are obtained. From this figure it can be seen that the position signatures under load can deviate significantly from the unloaded signature.

The influence of cross-saturation on the voltage waveforms for  $\theta = 60^\circ$ , corresponding to the aligned position with respect to phase  $B$ , are shown in Fig. 5. It can be seen that the resonance frequency increases with increasing current level in the active phase. This is consistent with the expectation that cross-saturation leads to a decreased inductance of phase  $C$ . If the different resonances are sampled at time  $t_s$ , this results in decreasing voltage samples with increasing load current.

From Fig. 4 it can be seen that cross-saturation has an important impact on the position signature in the interval  $[26^\circ-56^\circ]$ , which is used for position sensing. This is due to the fact that the mutual coupling between phases  $B$  and  $C$  is relatively large in this interval. For rotor angles outside this interval, cross-saturation has a smaller impact on the position signature. Therefore, the influence of cross-saturation is smaller in the case that the machine is used as a generator; to produce a breaking torque, phase  $B$  would normally be excited in the interval where its inductance is decreasing. In Figs. 3 and 4, this would correspond with the interval  $[64^\circ-94^\circ]$ .

For motoring operation however, cross-saturation has an important impact on the position signature. If commutation

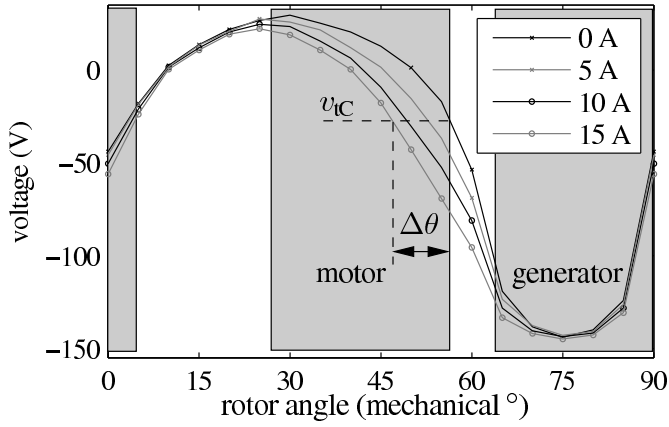


Figure 4. Effect of cross-saturation on the position signature of phase  $C$ . The current in phase  $B$  is controlled at constant values of 0, 5, 10 and 15 A.

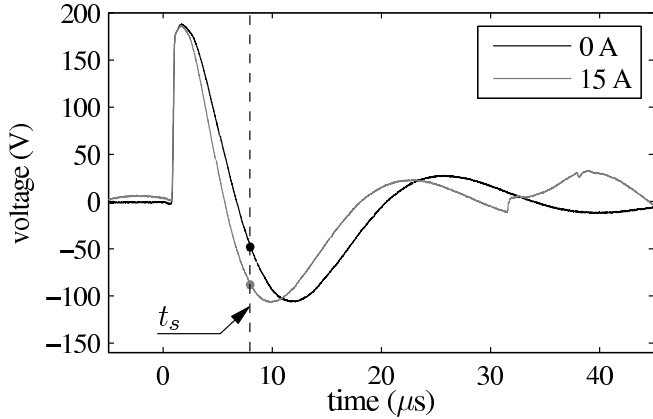


Figure 5. Effect of cross-saturation on voltage resonances of phase  $C$ . Phase  $B$  is aligned ( $\theta = 60^\circ$ ); the current  $i_b$  is controlled at a constant value of 0 and 15 A.

should be performed at  $56^\circ$ , the voltage threshold  $v_{tC}$  can be used as a commutation criterion, see Fig. 4. However, if phase  $C$  carries the rated current, the position signature crosses the threshold  $v_{tC}$  at a rotor angle of  $46^\circ$ , instead of  $56^\circ$  at no-load. The resulting position error  $\Delta\theta_c$  of 10 mechanical degrees is in most cases unacceptable.

#### IV. CROSS-SATURATION COMPENSATION SCHEME

As discussed in the previous section, cross-saturation leads to a voltage deviation in the phase signature, and thus to a position estimation error. Fig. 6 shows the voltage deviation, obtained by subtraction of the cross-saturated phase  $C$  signatures with the no-load signature.

Ideally, the commutation angle error can be reduced to zero if the no-load commutation threshold voltage  $v_{tC}$  is augmented with the current-dependent voltage deviation at  $56^\circ$ . However, a locked-rotor test is required to determine  $\Delta v_{sC}$  at the commutation position  $56^\circ$  for different  $i_b$ .

An alternative approach is that  $\Delta v_{sC}(56^\circ, i_b)$  is predicted by means of a measurement of  $\Delta v_{sC}(60^\circ, i_b)$ . No locked-

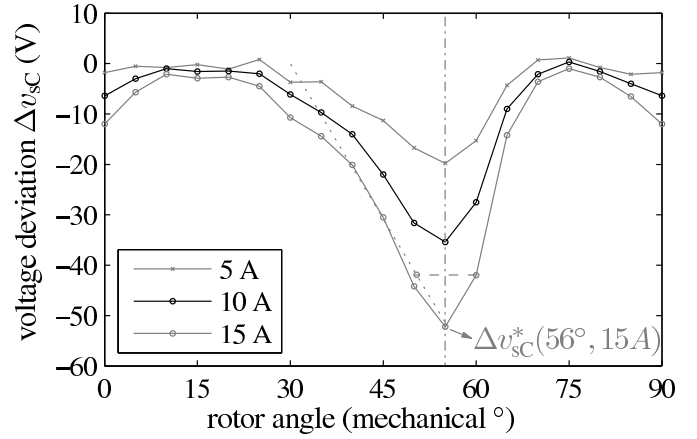


Figure 6. Voltage deviation  $\Delta v_{sC}$  between phase  $C$  position signatures at 5, 10, 15 A with signature at zero-current. The dotted line indicates the interpolation method to obtain the approximated voltage deviation  $\Delta v_{sC}^*(56^\circ)$  for  $i_b = 15$  A.

rotor test is required in this case, as the rotor automatically aligns at this position when current flows in phase  $B$ . From Fig. 6 it can be seen that the voltage deviation curves show more or less symmetry with respect to (and in close vicinity to) the position  $55^\circ$ . Therefore, the voltage deviation at  $50^\circ$  approximates the measured voltage deviation at  $60^\circ$ . For a known value  $\Delta v_{sC}(60^\circ, i_b)$ , the estimated voltage deviation  $\Delta v_{sC}^*(\theta, i_b)$  can be obtained by means of a linear interpolation:

$$\Delta v_{sC}^*(\theta, i_b) = \frac{\theta - 30}{50 - 30} \Delta v_{sC}(60^\circ, i_b). \quad (3)$$

Fig. 6 indicates the interpolation for the case of  $i_b = 15$  A. It can be seen that the interpolation yields a good approximation for the voltage deviation  $\Delta v_{sC}^*(\theta, 15$  A) in a range of rotor angles between  $40^\circ$  and  $56^\circ$ . This implies that cross-saturation effects can be taken into account when detecting both low-speed and high-speed (advanced) commutation angles.

In order to apply (3),  $\Delta v_{sC}(60^\circ, i_b)$  has to be known for a range of currents  $i_b$ . This current-dependency is almost linear, as shown in Fig. 7. Therefore, an interpolation can be used, based on the measurement of  $\Delta v_{sC}(60^\circ)$  at one specific current level, e.g. the rated current  $i_b = 15$  A:

$$\Delta v_{sC}(60^\circ, i_b) = \Delta v_{sC}(60^\circ, 15 \text{ A}) \cdot \frac{i_b}{15 \text{ A}}, \quad (4)$$

The presented interpolation schemes (3) and (4) give a good approximation for the voltage deviation at varying commutation positions, as will be shown in the experimental results.

Based on the previous discussion it can be concluded that the cross-saturation compensation scheme requires (apart from the no-load phase position signatures of Fig. 3) one extra parameter per phase. In the case of phase  $C$ , this is the voltage deviation  $\Delta v_{sC}(60^\circ, 15$  A). This value can be measured by controlling the current in phase  $B$  at 15 A and measuring the resonance voltage in phase  $C$  after the rotor has aligned itself.

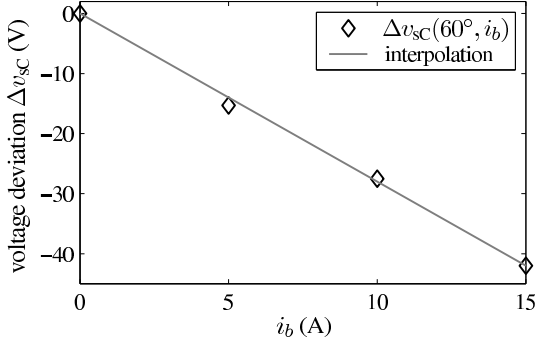


Figure 7. Dependence of voltage deviation samples  $\Delta v_{sc}(60^\circ)$  on  $i_b$ .

## V. EXPERIMENTAL VALIDATION

For the experimental validation the switched reluctance motor under test is coupled to a permanent-magnet synchronous machine (PMSM). The SRM is operated with current control, which is equivalent to torque control. The PMSM is operated in speed-control mode. A fixed speed command is given to the PMSM. While the PMSM is rotating at constant speed, the SRM receives a current command which increases gradually from zero to rated current. At rated current 15 A, the SRM generates a torque of 15 Nm. The SRM operates as a motor, delivering the demanded torque, while the PMSM operates as a generator, maintaining the speed at the predetermined level.

The desired commutation angle for the SRM is speed-dependent. At low speed commutation from phase *B* to phase *A* should take place at  $\theta_c = 56^\circ$ . At higher speeds a phase advance angle is calculated based on the time required by the current to rise to its set value between the turn-on angle and the static commutation angle  $26^\circ$ . This time can be calculated from

$$V_{dc} = L_u di/dt, \quad (5)$$

in which  $V_{dc}$  is the bus bar voltage and  $L_u$  is the unaligned phase inductance. For a given speed  $\omega$  the phase advance angle can then be calculated with

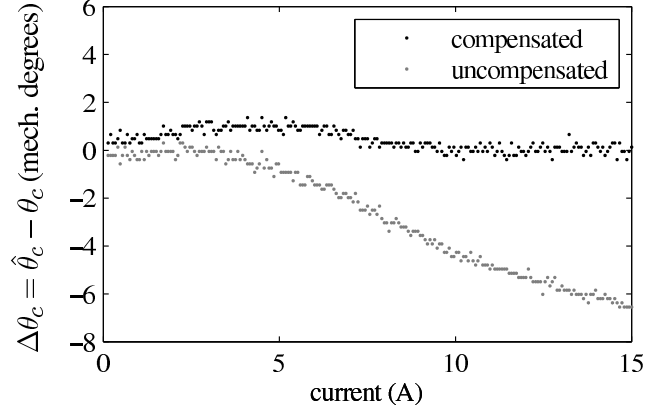
$$\theta_a = \omega \Delta t = \omega L_u \Delta i / V_{dc}. \quad (6)$$

With the values  $V_{dc} = 200$  V and  $L_u = 13$  mH, the desired commutation angle is given by

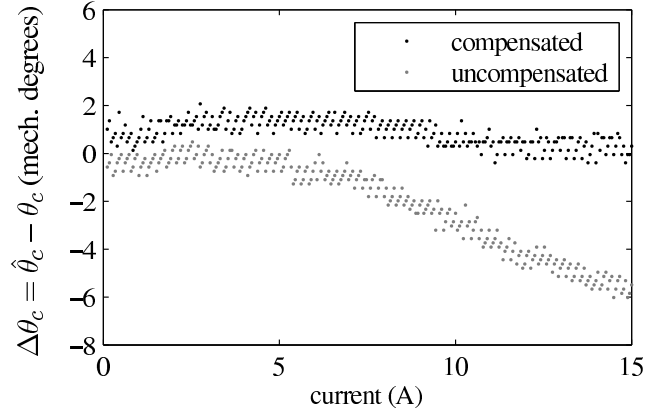
$$\theta_c = 56^\circ - \theta_a = 56^\circ - 6.5 \cdot 10^{-5} \omega \Delta i. \quad (7)$$

During sensorless operation, the commutation instants for the SRM are estimated according to the following algorithm, which is executed in each PWM period of  $250 \mu s$ . The algorithm is described for the case that phase *B* is the active phase and phase *C* is the test phase.

- 1) Measurement of resonance voltage  $v_c$  and current  $i_b$ .
- 2) Determination of no-load commutation threshold voltage  $v_{sc}(\theta_c)$  from phase *C* position signature, see Fig. 3.
- 3) Estimation of voltage deviation  $\Delta v_{sc}^*(\theta_c, i_b)$  by means of the interpolation schemes (3) and (4).
- 4) Commutation if  $v_c < v_{sc}(\theta_c) + \Delta v_{sc}^*(\theta_c, i_b)$ .



(a) Speed 150 r/min; desired commutation angle  $\theta_c = 55.1^\circ$  at 15 A.



(b) Speed 600 r/min; desired commutation angle  $\theta_c = 52.5^\circ$  at 15 A.

Figure 8. Phase *C* commutation position error as a function of the current in phase *B*.

For each commutation during the ramp-up of the torque command, the rotor angle  $\hat{\theta}_c$  is measured with an encoder and compared with the desired (speed and load dependent) commutation angle  $\theta_c$ . The resulting commutation position errors are shown in Figs. 8(a) and 8(b) for a speed of 150 r/min and 600 r/min respectively. The figures also show the position errors in the case that no cross-saturation compensation scheme is provided.

From both figures it can be seen that the cross-saturation compensation scheme keeps the position estimation error below 2 degrees over the rated load range. On the other hand, if no compensation for cross-saturation is performed, the position error gradually increases to an unacceptable value of more than 6 mechanical degrees, leading to a significant torque reduction. During short-term overloads of the machine, the error is expected to increase even more.

The figures also show that the 'noise' on the position error samples is larger at 600 r/min. This is due to the fact that only one voltage resonance is triggered in each PWM period of  $250 \mu s$ . Hence, the variation on the estimated commutation angle becomes larger at higher speeds.

## VI. CONCLUSION

A sensorless resonance-based commutation scheme is presented which takes into account cross-saturation between phases of a switched reluctance machine. The scheme requires only one additional parameter per phase which can be easily measured by a commissioning algorithm, without the need for a locked-rotor test. The scheme yields a position estimation error below 2 mechanical degrees over the rated load range. Experimental results at low and medium speed are presented.

## REFERENCES

- [1] I. Husain and M. Ehsani, "Rotor position sensing in switched reluctance motor drives by measuring mutually induced voltages," *IEEE Trans. Ind. Appl.*, vol. 30, no. 3, pp. 665–672, May/Jun. 1994.
- [2] W. D. Harris and J. H. Lang, "A simple motion estimator for variable-reluctance motors," *IEEE Trans. Ind. Appl.*, vol. 26, no. 2, pp. 237–243, Mar./Apr. 1990.
- [3] J. Lyons, S. MacMinn, and M. Preston, "Flux-current methods for SRM rotor position estimation," in *Conference Record of the IEEE Industry Applications Society Annual Meeting*, vol. 1, 28 Sep–4 Oct 1991, pp. 482–487.
- [4] I. St. Manolas, A. Kladas, and S. Manias, "Finite-element-based estimator for high-performance switched reluctance machine drives," *IEEE Trans. Magn.*, vol. 45, no. 3, pp. 1266–1269, Mar. 2009.
- [5] Y. Liu and P. Pillay, "Improved torque performance of switched reluctance machines by reducing the mutual saturation effect," *IEEE Trans. Energy Convers.*, vol. 19, no. 2, pp. 251–257, Jun. 2004.
- [6] K. R. Geldhof, A. Van den Bossche, and J. A. A. Melkebeek, "Rotor position estimation of switched reluctance motors based on damped voltage resonance," *IEEE Trans. Ind. Electron.*, accepted for publication.